D-salicin induces oxidative stress-mediated ERK1/2 suppression and apoptosis in endometrial cancer cells

NEZIHA SENEM ARI and AYŞE ÇAKIR GÜNDOĞDU

Department of Histology and Embryology, Faculty of Medicine, Kütahya Health Sciences University, Kütahya 43100, Türkiye

Received March 3, 2026; Accepted May 7, 2026

DOI: 10.3892/ol.2026.15666

Abstract. Endometrial cancer is a common gynecologic malignancy for which therapeutic options remain limited in advanced or treatment-resistant disease. Natural compounds that selectively perturb cancer-associated redox signaling and survival pathways may offer novel anticancer strategies. The present study investigated the anticancer effects of D-salicin in the endometrial adenocarcinoma-derived Ishikawa cell line, with a focus on oxidative stress and extracellular signal-regulated kinase (ERK)1/2 signaling, and assessed cancer selectivity using normal human dermal fibroblasts (HDF). D-salicin selectively reduced Ishikawa cell viability in a concentration-dependent manner while largely sparing HDF. This cytotoxic effect was accompanied by marked intracellular reactive oxygen species (ROS) accumulation, increased lipid peroxidation (MDA) and depletion of total glutathione (GSH), indicating induction of oxidative stress. Elevated oxidative burden was associated with caspase-3 activation and concentration-dependent suppression of ERK1/2 phosphorylation, both of which were attenuated by N-acetylcysteine (NAC) co-treatment. To determine redox dependence, NAC was incorporated as an antioxidant co-treatment. D-salicin induced a significant, concentration-dependent reduction in Ishikawa cell viability ($P<0.0001$), whereas HDF viability remained largely preserved across the tested range ($P>0.05$). In Ishikawa cells, D-salicin markedly increased intracellular ROS in a dose-dependent manner ($P\leq0.01$) and this effect was markedly attenuated by NAC co-treatment ($P\leq0.01$), indicating an NAC-sensitive oxidative component. Consistent with redox disruption, D-salicin increased MDA levels and depleted total GSH in Ishikawa cells ($P\leq0.01$). Elevated oxidative stress was accompanied by increased caspase-3 levels ($P\leq0.01$), supporting engagement of apoptotic signaling. Moreover, D-salicin markedly suppressed ERK1/2 phosphorylation in Ishikawa cells ($P<0.0001$), while ERK signaling was not markedly altered in HDF cells ($P>0.05$). Notably, NAC co-treatment partly restored p-ERK1/2 levels under the IC_{50} condition ($P<0.01$ vs. D-salicin alone), supporting a redox-linked contribution to ERK pathway modulation. Collectively, these findings indicated that D-salicin exerts selective anticancer effects in endometrial cancer cells by inducing oxidative stress and disrupting ERK1/2-mediated survival signaling, with NAC-sensitive modulation consistent with involvement of a redox-responsive ROS-ERK axis.

Introduction

Endometrial cancer is among the most common gynecologic malignancies affecting women worldwide, with ~417,000 new cases and 97,000 deaths recorded globally in 2020 alone, and its incidence continues to rise steadily. Recent global cancer statistics indicate that this increase is largely driven by aging populations, rising obesity rates and lifestyle-associated risk factors (1,2). Although prognosis is generally favorable when endometrial cancer is diagnosed at an early stage, the therapeutic landscape for advanced, recurrent, or treatment-resistant disease remains limited, with poor long-term outcomes despite multimodal treatment approaches (3). These challenges highlight the need to identify novel agents capable of targeting key molecular vulnerabilities in endometrial cancer cells.

Reactive oxygen species (ROS) have emerged as central regulators of cancer cell biology, functioning as both signaling mediators and inducers of cellular damage. Evidence emphasizes the dual role of ROS: While moderate ROS levels may support proliferation and adaptive signaling, excessive ROS accumulation disrupts redox homeostasis, promotes mitochondrial dysfunction and triggers apoptotic cell death (4,5). Importantly, redox alterations are tightly interconnected with mitogen-activated protein kinase (MAPK) signaling, particularly the extracellular signal-regulated kinase (ERK1/2) pathway. Dysregulated ERK1/2 activation contributes to enhanced proliferation, survival signaling, and therapeutic resistance in multiple malignancies, including endometrial carcinoma (6,7). Accordingly, the ROS-ERK axis is increasingly recognized as a critical determinant of cancer cell fate and a promising therapeutic target.

Correspondence to: Dr Neziha Senem Arı, Department of Histology and Embryology, Faculty of Medicine, Kütahya Health Sciences University, Evliya Çelebi Campus, Tavşanlı Road 10th km, Kütahya 43100, Türkiye
E-mail: nezihasenem.ari@ksbu.edu.tr

Key words: D-salicin, endometrial cancer, reactive oxygen species, extracellular signal-regulated kinase 1/2, N-acetylcysteine, apoptosis, oxidative stress

Natural phenolic compounds have attracted sustained interest in cancer research due to their capacity to modulate oxidative stress and intracellular signaling networks across multiple tumor types, including breast, colorectal, lung and gynecologic cancers. Plant-derived phenolic compounds can influence MAPK/ERK signaling, often through ROS-dependent mechanisms, thereby suppressing tumor cell proliferation and promoting cell death (8). Salicin, a phenolic glycoside traditionally isolated from willow bark, has a long history of pharmacological relevance and has recently gained renewed attention for its potential anticancer properties. Modern formulation strategies, including salicin-based nanocarriers and other phytochemical nano-delivery systems, have demonstrated improved cytotoxic and antiproliferative effects in cancer cell models through enhanced bioavailability, targeted delivery, and redox-mediated mechanisms (9). In addition, structural derivatives of salicin, such as salicin dimethyl ether, have been shown to inhibit tumor cell proliferation and induce apoptotic signaling (10).

Importantly, mechanistic studies have provided evidence that salicin and certain salicin derivatives can modulate intracellular redox status and ERK-related signaling. For example, salicin has been reported to inhibit angiogenesis via blockade of the ROS-ERK pathway (11). In addition, salicin dimethyl ether has been reported to exert inhibitory effects in laryngeal cancer cells through activation of apoptosis, supporting the plausibility that salicin-derived structures can engage stress-survival signaling nodes relevant to cancer cell fate (10). However, despite these insights, the effects of D-salicin on ROS production and ERK1/2 activity in gynecologic malignancies, especially endometrial cancer, remain insufficiently explored.

To evaluate the causal involvement of oxidative stress in D-salicin-induced cytotoxicity, antioxidant modulation strategies were incorporated into the experimental design. N-acetylcysteine (NAC), a well-established precursor of intracellular glutathione (GSH), acts as a thiol-based antioxidant and redox regulator (12,13). NAC is widely used in experimental cancer models to test whether ROS generation directly contributes to cytotoxic and apoptotic responses (14,15). By replenishing intracellular thiol pools and restoring redox homeostasis, NAC facilitates functional interrogation of ROS-dependent signaling pathways, including MAPK/ERK modulation (16). Accordingly, NAC co-treatment provides a pathway-level approach to assess whether D-salicin-induced ERK1/2 alterations and apoptotic responses are mediated by oxidative stress-dependent processes (15).

The present study investigated the anticancer effects of D-salicin in the endometrial adenocarcinoma-derived Ishikawa cell line. Cell viability was assessed using the MTT assay, apoptotic responses were quantified via caspase-3 ELISA, intracellular oxidative stress was measured through ROS assays, and changes in phospho-ERK1/2 expression were evaluated using immunofluorescence. In addition, NAC co-treatment experiments were conducted to examine whether restoration of intracellular redox balance modifies D-salicin-induced cytotoxicity and ERK1/2 signaling alterations. To the best of our knowledge, this is among the first studies of D-salicin-mediated ROS-ERK1/2 modulation in endometrial cancer cells using antioxidant-based functional validation. Through this integrated experimental approach, the present study aimed to elucidate whether D-salicin exerts its anticancer effects via activation of oxidative stress and modulation of the ROS-ERK1/2 signaling axis in endometrial cancer cells.

Materials and methods

Cell lines and culture conditions. The Ishikawa human endometrial adenocarcinoma cell line and human dermal fibroblasts (HDF; PCS-201-012) were obtained from the American Type Culture Collection (ATCC) and cultured according to the supplier's recommendations. HDF cells are non-immortalized normal human dermal fibroblasts and, under standard culture conditions, typically exhibit lower baseline proliferative activity and ERK1/2 signaling compared with actively dividing cancer cell lines, consistent with their non-malignant phenotype. All cells were maintained at 37˚C in a humidified atmosphere containing 5% CO_2 under standard culture conditions. Since commercially available ATCC cells were used, no additional ethical approval was required.

Assessment of cell viability by MTT. Cytotoxic responses to D-salicin were quantified using the MTT colorimetric assay. Ishikawa and HDF cells were seeded into 96-well plates and treated with escalating concentrations of D-salicin (0-80 μM) for 72 h. D-salicin stock solutions were prepared directly in complete culture medium, and no additional organic solvent was used. After incubation, MTT was added and allowed to metabolize for 4 h, generating formazan crystals, which were subsequently dissolved with dimethyl sulfoxide and quantified at 570 nm by a Multiskan FC Microplate Photometer (Thermo Fisher Scientific, Inc.). Each condition was assayed in technical triplicate, and experiments were independently repeated at least three times. Cell viability was expressed as a percentage of untreated control cells and dose-response curves were analyzed using nonlinear regression to calculate IC_{25}, IC_{50}, and IC_{75} values. To probe the contribution of oxidative stress to D-salicin-induced cytotoxicity, N-acetylcysteine (NAC) was included as an antioxidant co-treatment. To determine an NAC concentration suitable for use in both malignant and non-malignant cells without causing appreciable cytotoxicity, Ishikawa and HDF cells were exposed to NAC (0.5-10 mM) for 72 h and viability was assessed by MTT under the same conditions. The concentration used in subsequent co-treatment experiments was chosen based on this preliminary NAC screening. For NAC co-treatment experiments, cells were treated with D-salicin in the presence or absence of NAC for 72 h, after which MTT was performed as aforementioned. Untreated (vehicle control), D-salicin-treated, NAC-only and D-salicin + NAC co-treated wells were included to enable appropriate normalization and comparison of treatment effects.

Intracellular ROS measurement. Intracellular ROS levels were quantified using the DCFDA/H_2DCFDA Cellular ROS Assay Kit (Abcam; cat. no. ab113851) according to the manufacturer's guidelines, with minor adjustments for adherent cell cultures. Ishikawa and HDF cells were seeded into black-walled 96-well plates and allowed to attach overnight. Cells were then exposed to D-salicin at the previously determined IC_{25}, IC_{50} and IC_{75} concentrations for 72 h. In addition, cells were treated with 0.5 mM NAC concomitantly with D-salicin and incubated for

72 h. Untreated and NAC-only (0.5 mM) wells were included as negative controls, and a 200 μM H_2O_2 treatment for 30 min was used as a positive control.

Following treatment, the wells were washed once with Hank's Balanced Salt Solution (HBSS) and incubated with 20-25 μM DCFDA in HBSS for 30 min at 37˚C in the dark. After dye loading, the plates were washed again with HBSS, and fluorescence was recorded using a Varioskan (Varioskan Lux; Thermo Fisher Scientific, Inc.) microplate reader (Ex/Em=485/535 nm). Background fluorescence from blank wells was subtracted, and ROS levels were expressed as relative fluorescence units normalized to total protein content per well, determined using the BCA assay. Each condition was assayed in technical triplicate, and experiments were independently repeated at least three times.

Lipid peroxidation (MDA) and GSH quantification by ELISA. To further characterize D-salicin-associated oxidative stress at the levels of lipid peroxidation and antioxidant capacity, malondialdehyde (MDA) and GSH levels were quantified by ELISA. Ishikawa and HDF cells were treated with D-salicin at the previously determined IC_{25}, IC_{50} and IC_{75} concentrations for 72 h, alongside control wells. Following treatment, cells were washed with PBS, harvested, and lysed according to the manufacturers' sample preparation recommendations. Cell lysates underwent centrifugation at 10,000 x g for 10 min at 4˚C, and the resulting supernatants were used for analysis. MDA and GSH were measured using commercial ELISA kits (Elabscience; MDA ELISA Kit, cat. no. E-EL-0060; GSH ELISA Kit, cat. no. E-EL-0026) according to the manufacturers' instructions. Optical density was measured at 450 nm using a microplate reader (Varioskan Lux; Thermo Fisher Scientific, Inc.), and concentrations were calculated from the corresponding standard curves. MDA levels were reported as ng/ml and GSH levels as μg/ml. To allow comparability across wells, MDA and GSH values were normalized to total protein content determined by the BCA assay (reported as ng/mg protein and μg/mg protein, respectively). Each condition was assayed in triplicate, and the experiments were independently repeated at least three times (n=3 biological replicates).

Caspase-3 protein quantification by ELISA. Caspase-3 protein levels, used as an indicator of apoptosis, were quantified using the Human Caspase-3 ELISA Kit (BT Lab; cat. no. E4804Hu) according to the manufacturer's instructions. All reagents and samples were stored at 2-8˚C and equilibrated to room temperature before use. Cell lysates underwent centrifugation at 10,000 x g for 10 min at 4˚C, and the resulting supernatants were used for analysis. Standards and samples were added to 96-well plates, and the sandwich ELISA procedure, including antibody binding, incubation, and washing steps, was performed as recommended. Optical density was measured at 450 nm using a microplate reader (Varioskan Lux, Thermo Fisher Scientific, Inc.), and caspase-3 concentrations were calculated from the standard curve. Each condition was analyzed in triplicate, and the experiment was independently repeated at least three times.

Immunofluorescence staining of phospho-ERK1/2. Ishikawa and HDF cells were seeded onto sterile glass coverslips placed in 24-well plates at a density of $2x10^4$ cells/well and treated with D-salicin at IC_{25}, IC_{50}, and IC_{75} concentrations previously determined for Ishikawa cells for 72 h. For NAC co-treatment experiments, cells were treated concomitantly with 0.5 mM N-acetylcysteine (NAC) and D-salicin for 72 h. Following treatment, cells were washed twice with phosphate-buffered saline (PBS) and fixed with 4% paraformaldehyde for 15 min at room temperature. Fixed cells were permeabilized with 0.1% Triton X-100 in PBS for 10 min and blocked with 3% BSA; Sigma-Aldrich; cat. no. A9647) in PBS for 1 h at room temperature.. Cells were then incubated overnight at 4˚C with a rabbit polyclonal phospho-ERK1/2 (Thr202/Tyr204; Affinity Biosciences; cat. no. Ab-AF1015; 1:200) primary antibody. After three washes with PBS, cells were incubated with Alexa Fluor 594-conjugated goat anti-rabbit IgG (Jackson ImmunoResearch Laboratories, Inc.; cat. no. 111-585-003; 1:200) for 1 h at room temperature in the dark. Following the final washes, coverslips were mounted at room temperature using a DAPI-containing mounting medium (MilliporeSigma; cat. no. F6057), enabling simultaneous nuclear counterstaining.

Fluorescence images were acquired using a fluorescence microscope (Zeiss Calibri 7; Zeiss AG) under identical imaging parameters for all experimental groups. For quantitative analysis, fluorescence intensity measurements were performed using ImageJ software (version 2.16.0; National Institutes of Health). For each treatment concentration, at least three randomly selected microscopic fields were analyzed, and a minimum of 50 cells per field were evaluated to determine the mean fluorescence intensity of phospho-ERK1/2. Corrected total cell fluorescence (CTCF) values were calculated for each cell using the standard formula (CTCF=Integrated Density-[Area x Mean Background Fluorescence]) and analyzed as absolute fluorescence intensity measurements without normalization to a fixed reference value.

Statistical analysis. All quantitative data are presented as the mean ± standard deviation (SD) of at least three independent experiments (n≥3). Statistical analyses were performed using GraphPad Prism 8.4.2 (Dotmatics). Differences between groups were evaluated using one-way ANOVA) followed by Tukey's multiple comparisons test when more than two groups were compared. All graphs and statistical outputs were generated using GraphPad Prism. $P<0.05$ was considered to indicate a statistically significant difference.

Results

Cell viability. Treatment of Ishikawa cells with D-salicin for 72 h induced a concentration-dependent reduction in cell viability (Fig. 1A). While exposure to 10 μM D-salicin did not result in a statistically significant decrease compared with untreated cells, significant reductions in cell viability were observed starting from 20 μM. These reductions became progressively more marked at higher concentrations. The mean viability decreased from 100% in the control cells to ~16.9% at 80 μM D-salicin. Nonlinear regression analysis yielded an IC_{50} value of ~48.3 μM, with corresponding IC_{25} and IC_{75} values of 26.7 and 69.9 μM, respectively, indicating a marked cytotoxic effect of D-salicin on Ishikawa cells.

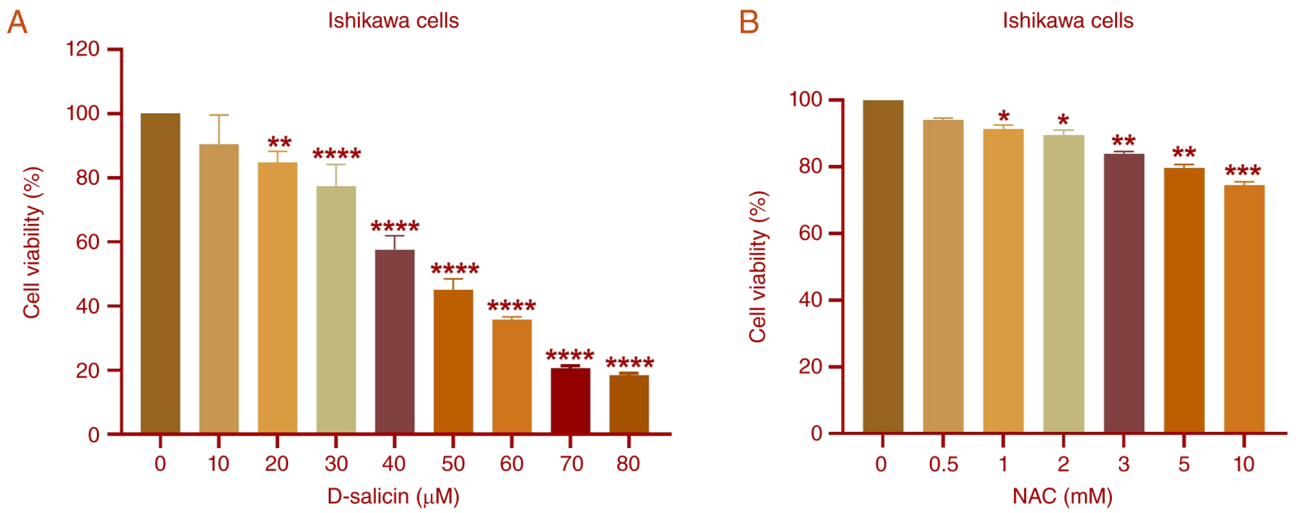

Figure 1. Effects of D-salicin and NAC on cell viability in Ishikawa cells. (A) Viability of Ishikawa cells following 72 h treatment with increasing concentrations of D-salicin (0-80 μM), as determined by the MTT assay. D-salicin induced a concentration-dependent decrease in cell viability. (B) Cell viability of Ishikawa cells following 72 h exposure to NAC (0.5-10 mM), as determined by the MTT assay. Data are expressed as percentage of control and presented as mean ± SD. Statistical analysis was performed using one-way ANOVA followed by Tukey's multiple comparisons test. *P<0.05, **P<0.01, ***P<0.001, ****P<0.0001. NAC, N-acetylcysteine.

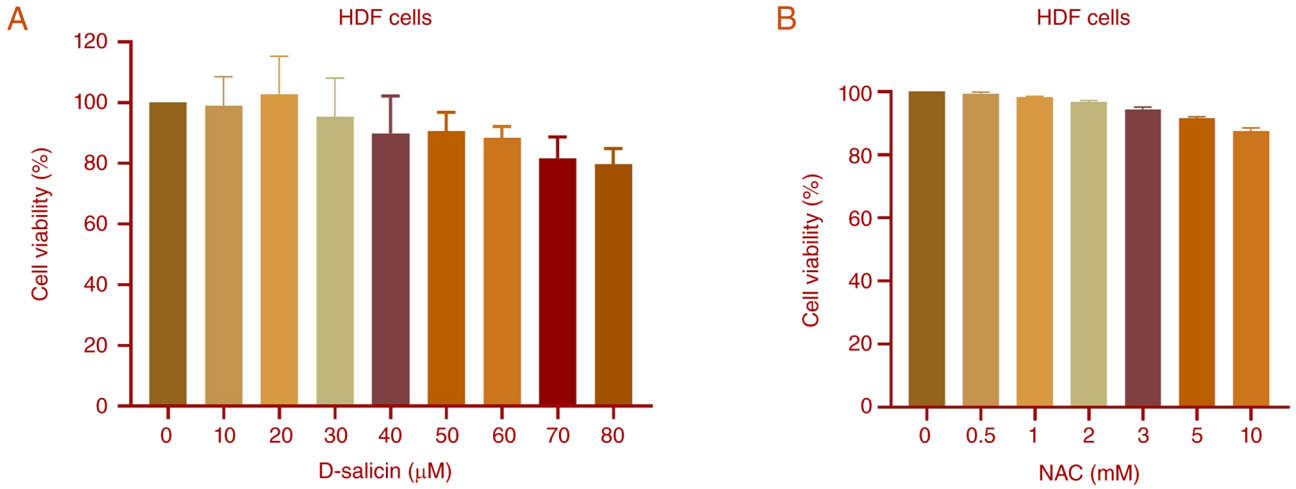

Figure 2. Effects of D-salicin and NAC on cell viability in HDF cells. (A) Cell viability of HDF cells following 72 h treatment with increasing concentrations of D-salicin (0-80 μM), as determined by the MTT assay. No significant reduction in viability was observed across the tested concentration range. (B) Cell viability of HDF cells following 72 h exposure to NAC (0.5-10 mM), as determined by the MTT assay. No significant reduction in viability was observed across the tested concentration range. NAC, N-acetylcysteine; HDF, human dermal fibroblasts.

To support selection of a sub-cytotoxic NAC concentration for subsequent co-treatment experiments, a preliminary NAC screening was performed in Ishikawa cells (Fig. 1B). At 0.5 mM NAC, viability did not markedly differ from control, whereas higher concentrations produced modest but significant reductions. Accordingly, 0.5 mM NAC was selected as a sub-cytotoxic concentration for subsequent co-treatment experiments. The slight (5-10%) reduction in cell viability observed at this concentration was not statistically significant and was therefore considered negligible; all subsequent experimental results were normalized to their respective control groups.

By contrast, HDF cells maintained relatively high viability across the same concentration range (0-80 μM) following 72 h of D-salicin treatment (Fig. 2A). Consistent with this, Shapiro-Wilk normality testing confirmed that all datasets followed a normal distribution. There were no significant differences between control and treatment groups, indicating that D-salicin did not significantly affect the viability of HDF cells under the experimental conditions. In addition, HDF cells exhibited minimal sensitivity to NAC across the tested range (Fig. 2B), with no statistically significant differences observed at any concentration, suggesting that NAC does not exert cytotoxic effects on HDF cells within the tested dose range. These findings suggested that D-salicin selectively reduces viability in Ishikawa endometrial cancer cells while exerting minimal cytotoxic effects on normal HDF cells.

Intracellular ROS levels. D-salicin treatment resulted in a significant and dose-dependent increase in intracellular ROS levels in Ishikawa endometrial cancer cells (Fig. 3A). When

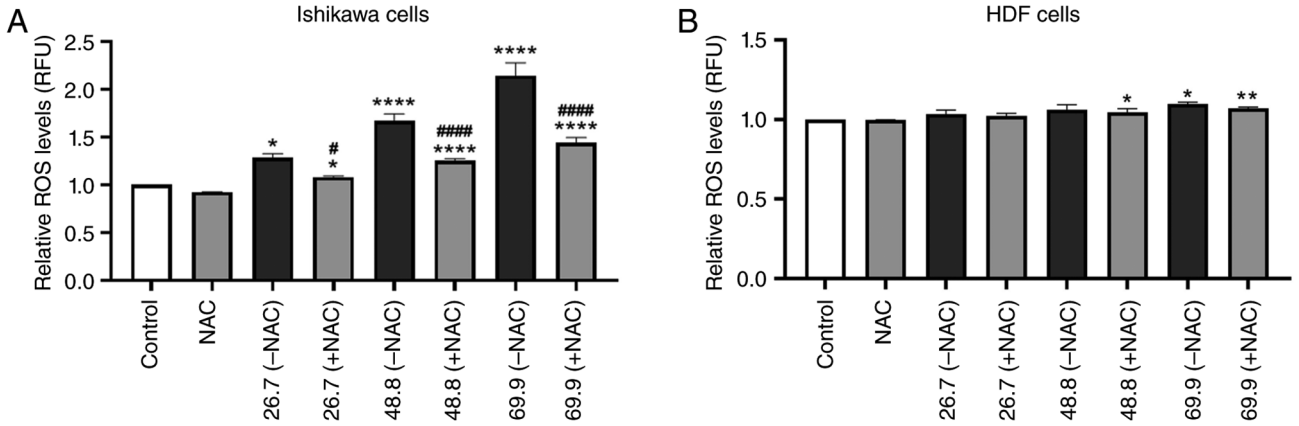

Figure 3. Effects of D-salicin and NAC co-treatment on intracellular ROS levels in Ishikawa and HDF cells. (A) Ishikawa cells and (B) HDF cells were treated with D-salicin at IC_{25} (26.7 μM), IC_{50} (48.8 μM), and IC_{75} (69.9 μM) for 72 h in the absence (-NAC) or presence (+NAC) of N-acetylcysteine (NAC, 0.5 mM). Control represents untreated cells, and NAC represents cells treated with NAC alone (0.5 mM). For D-salicin-treated groups, '-NAC' and '+NAC' indicate the absence or presence of NAC at each corresponding D-salicin concentration. Intracellular ROS levels were measured using the DCFDA assay and expressed as RFU, normalized to the untreated control. In Ishikawa cells, D-salicin induced a dose-dependent increase in ROS levels, which was markedly attenuated by NAC co-treatment. In HDF cells, D-salicin induced only modest changes in ROS levels, and NAC co-treatment did not markedly alter this response. Data are presented as mean ± SD (n≥3 independent experiments). Statistical analysis was performed using one-way ANOVA followed by Tukey's multiple comparisons test. Hash symbols (#) indicate comparisons between matched D-salicin groups in the absence and presence of NAC at the corresponding concentration [e.g., 26.7 (-NAC) vs. 26.7 (+NAC)]. *P<0.05, **P<0.01, ****P<0.0001 vs. untreated control; $^{\#}$P<0.05, $^{\#\#\#\#}$P<0.0001. NAC, N-acetylcysteine; ROS, reactive oxygen species; HDF, human dermal fibroblasts; RFU, relative fluorescence units.

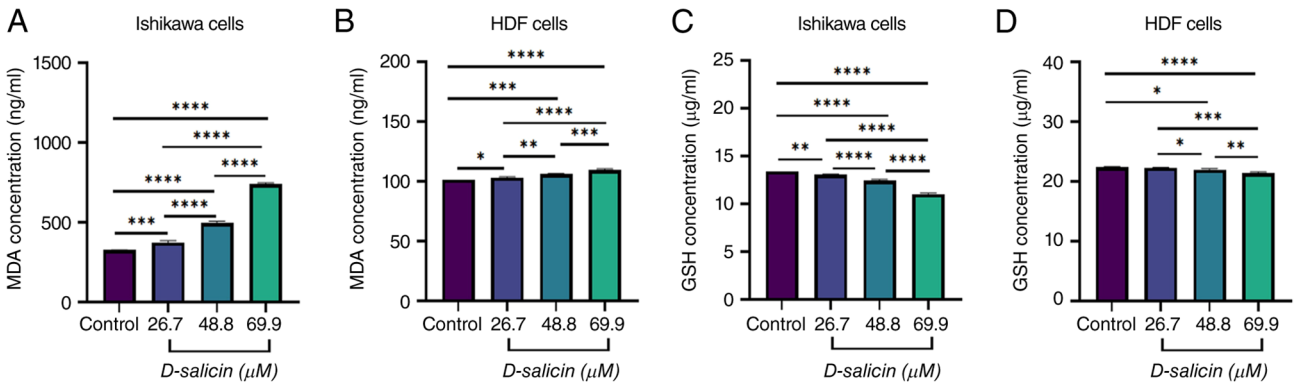

Figure 4. Effects of D-salicin on lipid peroxidation (MDA) and GSH levels in Ishikawa and HDF cells. (A) MDA concentrations in Ishikawa cells following 72 h exposure to D-salicin at IC_{25} (26.7 μM), IC_{50} (48.8 μM), and IC_{75} (69.9 μM). (B) MDA concentrations (ng/ml) in HDF cells under identical treatment conditions. (C) GSH concentrations (μg/ml) in Ishikawa cells following 72 h D-salicin exposure at IC_{25}, IC_{50}, and IC_{75}. (D) GSH concentrations (μg/ml) in HDF cells under identical conditions. MDA and GSH were quantified in cell lysates by ELISA, and concentrations were calculated from standard curves. Data are presented as mean ± SD from three independent experiments (n=3). Each condition was assayed in technical triplicate, and experiments were independently repeated at least three times (n≥3 biological replicates). Statistical analysis was performed using one-way ANOVA followed by Tukey's multiple comparisons test. *P<0.05, **P<0.01, ***P<0.001, ****P<0.0001. MDA, malondialdehyde; GSH, glutathione; HDF, human dermal fibroblasts.

normalized to the untreated control, ROS levels increased to 1.26-1.33-fold at 26.7 μM, 1.61-1.75-fold at 48.8 μM, and 2.00-2.28-fold at 69.9 μM D-salicin. All tested concentrations induced significant elevations compared with the control (Fig. 3A).

In the presence of NAC (+NAC), ROS levels at each D-salicin concentration remained significantly higher than in the control, although the magnitude of increase was consistently reduced compared with D-salicin treatment alone.

Direct comparisons between matched D-salicin concentrations in the absence and presence of NAC (26.7 vs. 26.7 + NAC; 48.8 vs. 48.8 + NAC; 69.9 vs. 69.9 + NAC) demonstrated a significant attenuation of ROS levels following NAC co-treatment. Despite this reduction, ROS levels in the NAC co-treatment groups remained moderately elevated relative to baseline at higher concentrations, indicating partial but not complete reversal of oxidative stress. NAC alone did not markedly alter ROS levels compared with the untreated control.

By contrast, HDF normal fibroblasts exhibited minimal changes in intracellular ROS levels following D-salicin exposure (Fig. 3B). Only the highest concentration (69.9 μM) induced a modest but statistically significant increase compared with control, while no significant differences were observed among lower concentrations. In the presence of NAC, ROS levels were modestly elevated at 48.8 and 69.9 μM compared with control. However, direct comparisons between D-salicin-treated groups in the absence and presence of NAC revealed no significant differences at any concentration.

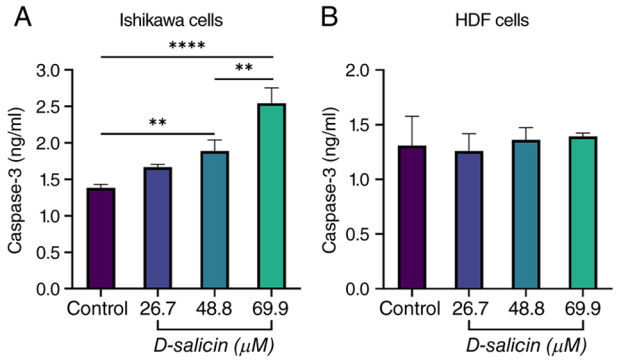

Figure 5. Effect of D-salicin on caspase-3 protein levels in Ishikawa and HDF cells. (A) Caspase-3 protein levels in Ishikawa cells following 72 h treatment with D-salicin at IC_{25} (26.7 μM), IC_{50} (48.8 μM), and IC_{75} (69.9 μM). D-salicin induced a concentration-dependent increase in caspase-3 levels. (B) Caspase-3 protein levels in HDF cells treated with D-salicin under identical conditions. No significant changes were observed across treatment groups. Data are presented as mean ± SD. Statistical analysis was performed using one-way ANOVA followed by Tukey's multiple comparisons test. $^{**}P<0.01$, $^{****}P<0.0001$. HDF, human dermal fibroblast.

These results indicated that D-salicin preferentially induces oxidative stress in Ishikawa cancer cells, with limited effects on normal fibroblasts.

Lipid peroxidation and GSH levels. D-salicin-associated oxidative stress was further evaluated by measuring lipid peroxidation (MDA) and GSH) levels in cell lysate after 72 h exposure to IC_{25} (26.7 μM), IC_{50} (48.8 μM), and IC_{75} (69.9 μM) concentrations (Fig. 4A-D).

In Ishikawa cells, D-salicin induced a marked, concentration-dependent increase in MDA concentrations (Fig. 4A). Compared with control, MDA levels were significantly elevated at 26.7 μM and increased further at 48.8 and 69.9 μM. Pairwise comparisons confirmed a progressive rise in lipid peroxidation between successive doses.

In HDF cells, MDA concentrations also increased following D-salicin exposure, although the magnitude of change was more modest than in Ishikawa cells (Fig. 4B). Relative to control, significant increases were observed at 26.7 48.8 and 69.9 μM, indicating that D-salicin can induce lipid peroxidation in normal fibroblasts, albeit to a lesser extent.

Conversely, GSH levels in Ishikawa cells decreased markedly and in a dose-dependent manner following D-salicin treatment (Fig. 4C). Compared with control, GSH concentrations were reduced at 26.7 μM and decreased further at 48.8 and 69.9 μM, with pairwise comparisons indicating greater depletion at higher concentrations.

In HDF cells, GSH levels showed a small but statistically significant reduction following D-salicin exposure (Fig. 4D). Compared with control, significant decreases were detected at 48.8 and 69.9 μM, whereas no significant change was observed at 26.7 μM. However, the absolute magnitude of GSH depletion was limited compared with Ishikawa cells, consistent with a comparatively attenuated redox disruption in normal fibroblasts.

Collectively, these results indicated that D-salicin promotes oxidative stress characterized by increased lipid peroxidation (MDA) and depletion of the antioxidant pool (GSH). The overall redox imbalance was more pronounced in Ishikawa cancer cells, supporting preferential disruption of redox homeostasis in the malignant cell model under identical exposure conditions. Although D-salicin also induced modest but statistically significant changes in MDA and GSH levels in HDF cells (Fig. 4B and D), these oxidative changes in HDF cells were not accompanied by significant reductions in cell viability or caspase-3 activation. This suggests that normal fibroblasts retain sufficient redox buffering capacity to tolerate D-salicin-induced oxidative perturbations without engaging cytotoxic or apoptotic programs, supporting a degree of functional selectivity even in the presence of partial oxidative stress induction in non-malignant cells.

Caspase-3 response to D-salicin exposure. In Ishikawa endometrial cancer cells, D-salicin treatment induced a concentration-dependent increase in caspase-3 protein levels (Fig. 5A). Compared with control cells, exposure to 26.7 μM D-salicin did not result in a statistically significant change. However, treatment with 48.8 μM led to a significant elevation in caspase-3, while the highest concentration (69.9 μM) produced a pronounced and highly significant increase. Pairwise comparisons among D-salicin-treated groups further demonstrated that caspase-3 levels at 69.9 μM were significantly higher than those observed at 26.7 and 48.8 μM. No significant difference was detected between the 26.7 and 48.8 μM treatment groups, indicating that apoptotic activation became more prominent at higher D-salicin concentrations. By contrast, HDF cells exhibited no statistically significant changes in caspase-3 protein levels following D-salicin treatment at any concentration tested (Fig. 5B). These findings suggested that D-salicin selectively activates caspase-3-associated apoptotic signaling in Ishikawa cancer cells while sparing normal fibroblasts.

Effect of D-salicin on ERK1/2 phosphorylation in Ishikawa and HDF cells. Immunofluorescence analysis revealed a marked, concentration-dependent suppression in ERK1/2 phosphorylation in Ishikawa cells following D-salicin treatment (Fig. 6A). In control Ishikawa cells, phosphorylated (p)-ERK1/2 immunoreactivity was prominently detected throughout the cytoplasm and nucleus. Treatment with D-salicin resulted in a progressive reduction in p-ERK1/2 fluorescence intensity, particularly at higher concentrations.

p-ERK1/2 fluorescence intensity was not markedly altered at 26.7 μM compared with control (Fig. 6A). However, treatment with 48.8 and 69.9 μM D-salicin led to a significant decrease in p-ERK1/2 levels relative to control (Fig. 6A). In addition, p-ERK1/2 intensity at 69.9 μM was significantly lower than at 26.7 μM and a modest but significant difference was also observed between 26.7 and 48.8 μM (Fig. 6A). No significant difference was detected between 48.8 μM and 69.9 μM (Fig. 6A), suggesting a plateau effect at higher concentrations.

By contrast, D-salicin treatment did not induce significant changes in ERK1/2 phosphorylation in HDF cells. Basal p-ERK1/2 expression was detectable but relatively low in HDF cells; however, it remained stable and did not show significant modulation upon D-salicin treatment. Immunofluorescence images showed consistently low p-ERK1/2 signal intensity

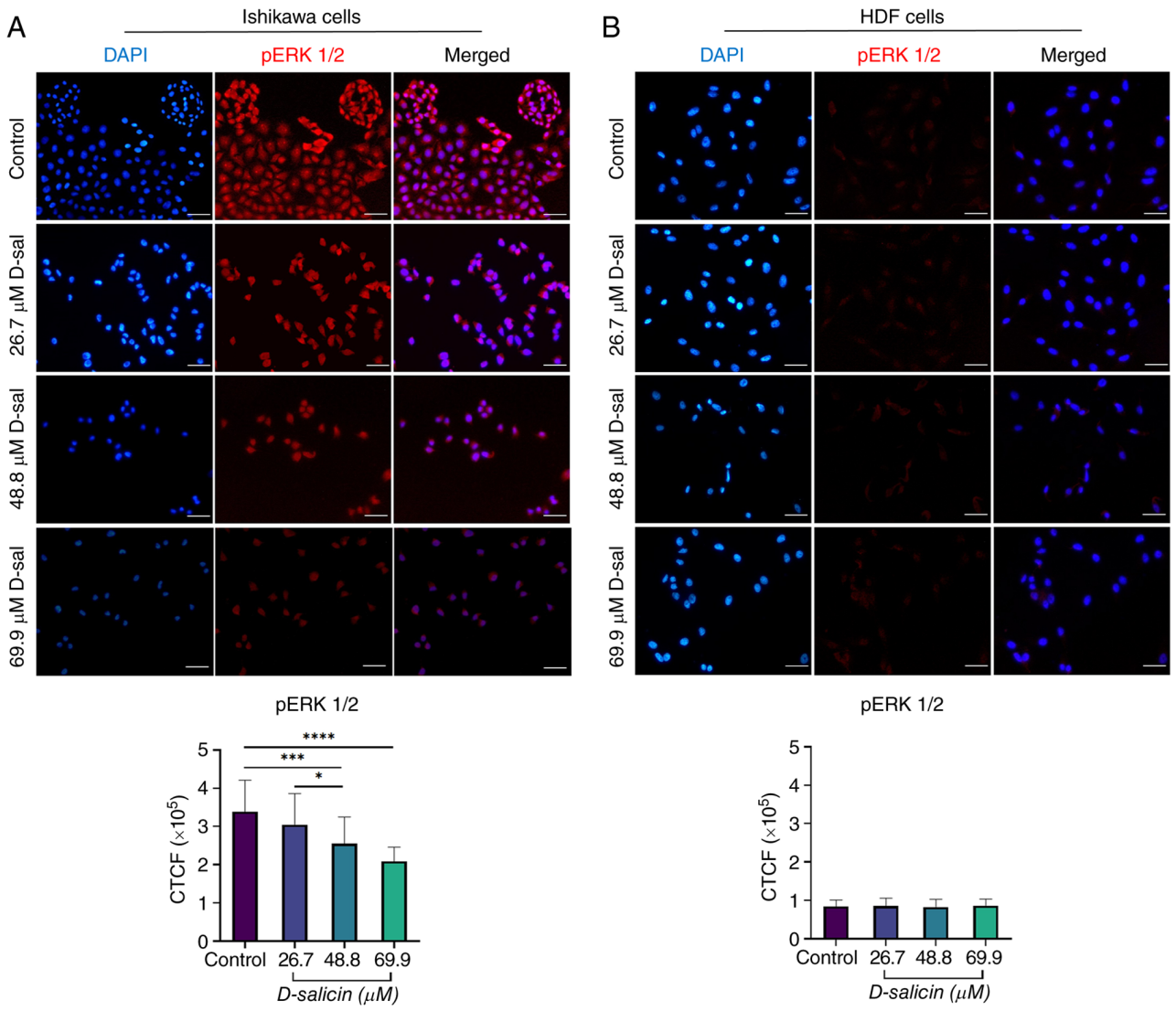

Figure 6. Effect of D-salicin on ERK1/2 phosphorylation in Ishikawa and HDF cells. (A) Representative immunofluorescence images of p-ERK1/2 expression in Ishikawa cells treated with D-salicin (26.7, 48.8, and 69.9 μM). p-ERK1/2 immunoreactivity (red) decreased in a concentration-dependent manner compared with control cells. Nuclei were counterstained with DAPI (blue). (B) Representative immunofluorescence images of HDF cells following D-salicin treatment under identical conditions. No apparent changes in p-ERK1/2 fluorescence intensity were observed across treatment groups. These representative immunofluorescence images are shown alongside the corresponding quantitative analysis to illustrate the observed changes in p-ERK1/2 expression. Bar graphs show quantitative analysis of p-ERK1/2 fluorescence intensity. Data are presented as mean ± SD. Statistical significance was determined by one-way ANOVA followed by Tukey's multiple comparisons test (*P<0.05, ***P<0.001, ****P<0.0001). Scale bar, 100 μm. CTCF values were calculated as absolute fluorescence intensity measurements, and statistical comparisons were performed directly between groups. p-, phosphorylated; CTCF, corrected total cell fluorescence.

across all treatment groups, and quantitative analysis confirmed the absence of statistically significant differences between control and D-salicin-treated HDF cells at any concentration tested (Fig. 6B).

To further examine whether D-salicin-induced suppression of ERK1/2 phosphorylation is linked to oxidative stress, NAC co-treatment experiments were performed using D-salicin at its IC_{50} concentration (48.8 μM) in Ishikawa cells (Fig. 7A and B). In these experiments, cells were treated with NAC alone (0.5 mM), D-salicin alone (48.8 μM), or D-salicin + NAC (0.5 mM), and p-ERK1/2 immunofluorescence intensity was quantified by CTCF. NAC alone did not significantly alter p-ERK1/2 levels compared with control. By contrast, D-salicin significantly reduced p-ERK1/2 intensity relative to control. Importantly, NAC co-treatment partially restored p-ERK1/2 phosphorylation compared with D-salicin alone, indicating that the ERK1/2 phosphorylation changes induced by D-salicin are at least partly NAC-sensitive under these conditions.

Collectively, these findings indicated that D-salicin selectively suppresses ERK1/2 phosphorylation in Ishikawa endometrial cancer cells in a concentration-dependent manner, while sparing ERK signaling in non-tumorigenic HDF cells. NAC co-treatment attenuated D-salicin-associated p-ERK1/2 suppression in Ishikawa cells, supporting a redox-linked (ROS-dependent) contribution to ERK pathway modulation under these conditions.

Discussion

The observed concentration-dependent reduction in Ishikawa cell viability, contrasted with the preserved viability of HDF

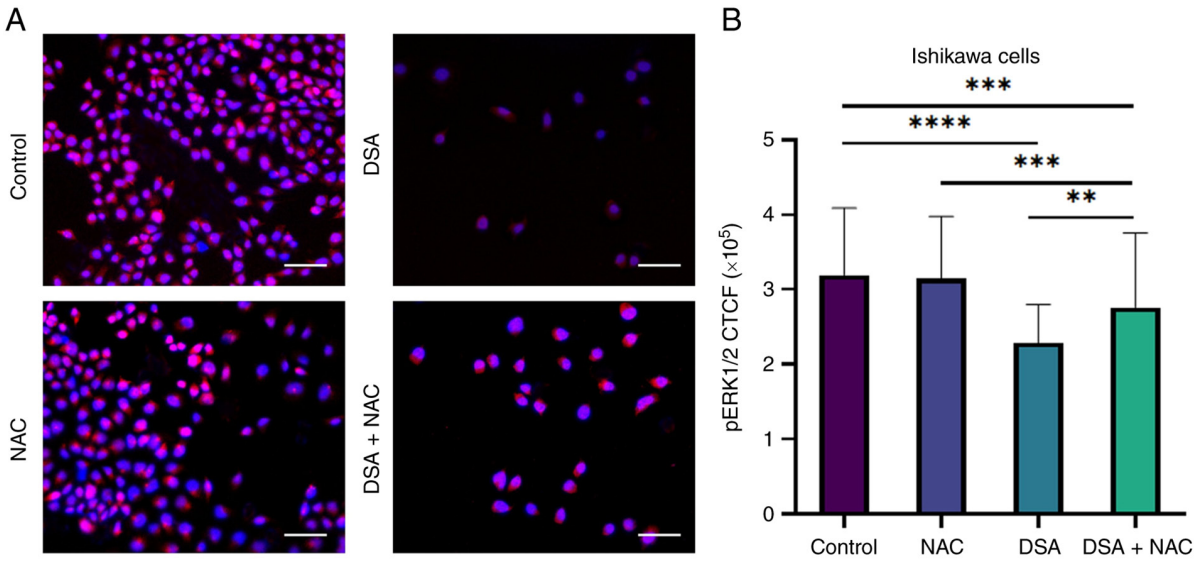

Figure 7. Effect of NAC co-treatment on D-salicin-induced suppression of ERK1/2 phosphorylation in Ishikawa cells. (A) Representative immunofluorescence images showing phospho-ERK1/2 (p-ERK1/2) expression in Ishikawa cells following 72 h treatment with control, NAC (0.5 mM), D-salicin (IC_{50}=48.8 μM), and D-salicin + NAC. p-ERK1/2 immunoreactivity is shown in red, and nuclei are counterstained with DAPI (blue). D-salicin reduced p-ERK1/2 fluorescence intensity compared with control, whereas NAC co-treatment partially restored p-ERK1/2 signal. (B) Quantitative analysis of p-ERK1/2 fluorescence intensity expressed as CTCF. Data are presented as mean ± SD from three independent experiments. Statistical significance was determined using one-way ANOVA followed by Tukey's multiple comparisons test **P<0.01, ***P<0.001, ****P<0.0001). Scale bars, 100 μm. NAC, N-acetylcysteine; p-, phosphorylated; CTCF, corrected total cell fluorescence; DSA, D-salicin.

cells, suggests a degree of tumor selectivity. Such selective cytotoxicity is a critical feature for candidate anticancer agents, because clinical efficacy is frequently constrained by dose-limiting toxicities in normal tissues and the need to widen the therapeutic window (17,18). This is particularly relevant in endometrial cancer, where advanced or recurrent disease remains therapeutically challenging and systemic treatment selection continues to evolve with histologic and molecular stratification (7,19). Although therapeutic options have expanded, improving response depth and durability, especially in microsatellite-stable disease, remains a major unmet need, supporting continued development of agents with novel mechanisms and favorable safety profiles (19,20). These challenges highlight the rationale for exploring redox-modulating compounds that exploit cancer-specific oxidative vulnerabilities to preferentially impact malignant cells (18,21).

ROS analyses indicated that D-salicin induces a robust and dose-dependent increase in intracellular oxidative stress in Ishikawa cells, whereas normal fibroblasts exhibited minimal ROS elevation. This finding aligns with the hypothesis that numerous cancer cells operate close to a redox 'tolerance limit,' making them more susceptible to additional oxidative insults than non-malignant cells (22). Salicylate/salicin-related natural products and willow-derived phenolics can influence intracellular redox balance and cancer-cell stress responses, supporting redox modulation as a plausible contribution to their bioactivity (23). Excessive ROS can overwhelm antioxidant defenses, promote mitochondrial dysfunction and precipitate regulated cell death programs (including apoptosis) when redox homeostasis collapses (24). In this context, ROS induction may represent an early event contributing to the anticancer activity of D-salicin by pushing malignant cells beyond their oxidative stress buffering capacity (22). Consistent with this interpretation, NAC co-treatment markedly blunted D-salicin-driven ROS accumulation across IC_{25}-IC_{75} conditions, supporting an NAC-sensitive oxidative component in Ishikawa cells. The differential ROS response between Ishikawa and HDF cells may reflect inherent differences in baseline antioxidant capacity and redox buffering between malignant and non-malignant cells. Cancer cells, including endometrial carcinoma lines, frequently exhibit elevated baseline ROS levels and reduced antioxidant reserves compared with normal counterparts, rendering them more susceptible to further oxidative insult. This concept of a redox 'threshold effect', whereby cancer cells operate closer to their oxidative tolerance limit, may explain the preferential ROS accumulation and downstream cytotoxic response observed in Ishikawa cells under identical D-salicin exposure conditions (22). Consistent with this interpretation, the present study demonstrated a more pronounced ROS elevation in Ishikawa cells compared with HDF cells under the same treatment conditions, supporting a tumor cell-specific redox vulnerability.

Consistent with ROS-mediated cytotoxicity, a significant increase in caspase-3 levels in Ishikawa cells at higher D-salicin concentrations was observed, indicating engagement of apoptotic execution pathways (25). Activation of caspase-3 represents a terminal step in the apoptotic cascade, leading to the proteolytic cleavage of essential cellular substrates and execution of cell death (26). Salicin/salicylate-related compounds can promote apoptotic cell death with caspase pathway involvement, often alongside oxidative stress signaling and suppression of pro-survival pathways (27). The absence of caspase-3 activation in HDF cells further underscores the cancer-selective pro-apoptotic effect of D-salicin and supports the interpretation that oxidative stress-induced apoptosis contributes to its anticancer activity (28). However,

while caspase-3 activation supports engagement of apoptotic signaling, it does not fully distinguish apoptosis from other antiproliferative mechanisms. Although caspase-3 was not evaluated under NAC co-treatment in the present dataset, the NAC-sensitive ROS and p-ERK1/2 responses are compatible with redox-dependent upstream events that can converge on apoptotic execution pathways (29). Importantly, although modest changes in oxidative stress markers were also observed in HDF cells, these effects were substantially less pronounced and were not associated with downstream cytotoxic or apoptotic responses, supporting a relative degree of tumor selectivity. Accordingly, the selectivity of D-salicin should be considered relative rather than absolute and interpreted within the context of differential cellular sensitivity to oxidative stress.

Immunofluorescence analysis revealed that D-salicin suppressed ERK1/2 phosphorylation in Ishikawa cells in a concentration-dependent manner, while ERK signaling remained largely unchanged in normal fibroblasts. The RAS-RAF-MEK-ERK (MAPK/ERK) cascade is a core signaling module that regulates cellular proliferation, growth, and survival, and dysregulated ERK1/2 activity is widely implicated in cancer progression and therapeutic resistance (6,30). Accordingly, the observed decrease in p-ERK1/2 in Ishikawa cells represents a disruption of pro-survival signaling that plausibly contributes to the cytotoxic response under D-salicin exposure. Notably, NAC co-treatment partly restored p-ERK1/2 levels at the IC_{50} condition, providing functional support that ERK suppression is at least partly redox-linked under these experimental conditions (13,31). It should be noted that the present study provided associative rather than direct mechanistic evidence for ROS-ERK coupling; NAC co-treatment offers functional support but does not exclude alternative upstream mediators. Complementary approaches, including pharmacological ERK activators or inhibitors and genetic modulation strategies, would be required to establish direct causality and will be addressed in future studies.

Collectively, the present data supported a model in which D-salicin elevated intracellular ROS levels beyond a tolerable threshold in endometrial cancer cells, leading to attenuation of ERK1/2-mediated survival signaling and activation of caspase-3-associated apoptotic signaling. The limited effects observed in normal fibroblasts suggest the existence of a therapeutic window, a desirable characteristic for further translational exploration. The observation that NAC attenuates D-salicin-induced ROS and partially reverses p-ERK1/2 suppression further supports involvement of a redox-sensitive ROS-ERK axis in the anticancer response.

From a translational perspective, the IC_{50} of D-salicin determined in the present study (~48 μM) warrants consideration in the context of physiological achievability. While *in vitro* IC_{50} values do not directly predict effective *in vivo* concentrations due to differences in bioavailability, protein binding and tissue distribution, the concentration range employed here was broadly comparable with those reported for other phenolic glycosides with demonstrated anticancer activity in cell-based models. However, it remains uncertain whether the IC_{50} concentration can be safely achieved *in vivo*. Nevertheless, *in vivo* pharmacokinetic and pharmacodynamic studies are required to evaluate whether therapeutically relevant plasma concentrations of D-salicin are achievable, and to assess its safety profile in more complex biological systems.

Several limitations of the present study should be acknowledged. First, the findings are based on *in vitro* analyses using a single endometrial cancer cell line; nevertheless, Ishikawa cells represent a well-established and widely used model of endometrial adenocarcinoma, supporting the biological relevance of the present findings within this system; therefore, validation in additional endometrial cancer models with distinct molecular backgrounds, such as HEC-1A or KLE cell lines representing different histologic and molecular subtypes, would strengthen generalizability. Second, although the present data indicated a strong association between ROS accumulation and ERK1/2 inhibition, complementary pharmacological and genetic approaches will be valuable to establish direct causal relationships. While NAC co-treatment provides functional support for redox involvement, additional strategies, such as alternative antioxidants/thiol modulators, ROS-generating controls, time-course experiments and direct manipulation of ERK signaling, would strengthen causal inference. Although NAC co-treatment was used to functionally assess redox involvement, direct measurement of GSH replenishment following NAC exposure was not performed and represents a limitation of the current study; future studies incorporating such analyses would further strengthen the interpretation of redox-related effects. Assessing apoptotic readouts (such as caspase-3 activity/cleavage or downstream substrates) under NAC co-treatment would further clarify whether redox modulation directly rescues apoptotic execution in this model. Moreover, caspase-3 ELISA reflects total protein levels rather than the cleaved/activated form; therefore, complementary approaches such as Annexin V-propidium iodide flow cytometry or PARP cleavage analysis would provide more definitive confirmation of apoptotic cell death. Such complementary approaches would also more precisely delineate the contribution of apoptosis vs. cell cycle arrest to the observed reduction in cell viability, particularly under NAC co-treatment conditions where ROS neutralization may engage distinct antiproliferative mechanisms.

Additionally, ERK1/2 phosphorylation was assessed by immunofluorescence, which provides spatial resolution but is semi-quantitative in nature; western blot analysis would offer complementary biochemical validation of the p-ERK1/2 findings reported here.

Finally, *in vivo* studies are required to evaluate the pharmacological feasibility, bioavailability, and safety profile of D-salicin, as well as to determine whether the observed redox-ERK modulation translates into antitumor efficacy in more complex biological systems.

In conclusion, this study provided evidence that D-salicin exerts selective anticancer effects in endometrial cancer cells through induction of oxidative stress, suppression of ERK1/2 signaling and activation of caspase-3-associated apoptotic signaling. The NAC-sensitive attenuation of ROS accumulation and partial restoration of p-ERK1/2 further implicate a redox-linked contribution to ERK pathway modulation. These findings position D-salicin as a promising

redox-modulating agent targeting the ROS-ERK axis in endometrial cancer.

Acknowledgements

Not applicable.

Funding

No funding was received.

Availability of data and materials

The data generated in the present study are included in the figures and/or tables of this article.

Authors' contributions

NSA and ACG conceived and designed the study. NSA supervised and coordinated the research. NSA and ACG conducted the experiments, performed the data analysis and interpreted the findings. NSA and ACG drafted the manuscript and critically revised it for important intellectual content. NSA and ACG confirm the authenticity of all the raw data. Both authors read and approved the final manuscript.

Ethics approval and consent to participate

Not applicable.

Patient consent for publication

Not applicable.

Competing interests

The authors declare that they have no competing interests.

Authors' information

Neziha Senem Arı ORCID ID 0000-0003-2926-6892. Ayşe Çakır Gündoğdu ORCID ID 0000-0002-2466-9417.

References

1. Sung H, Ferlay J, Siegel RL, Laversanne M, Soerjomataram I, Jemal A and Bray F: Global cancer statistics 2020: GLOBOCAN estimates of incidence and mortality worldwide for 36 cancers in 185 countries. CA Cancer J Clin 71: 209-249, 2021.
2. Bray F, Laversanne M, Sung H, Ferlay J, Siegel RL, Soerjomataram I and Jemal A: Global cancer statistics 2022: GLOBOCAN estimates of incidence and mortality worldwide for 36 cancers in 185 countries. CA Cancer J Clin 74: 229-263, 2024.
3. Concin N, Matias-Guiu X, Vergote I, Cibula D, Mirza MR, Marnitz S, Ledermann J, Bosse T, Chargari C, Fagotti A, *et al*: ESGO/ESTRO/ESP guidelines for the management of patients with endometrial carcinoma. Radiother Oncol 154: 327-353, 2021.
4. Panieri E and Santoro MM: ROS homeostasis and metabolism: A dangerous liaison in cancer cells. Cell Death Dis 7: e2253, 2016.
5. An X, Yu W, Liu J, Tang D, Yang L and Chen X: Oxidative cell death in cancer: Mechanisms and therapeutic opportunities. Cell Death Dis 15: 556, 2024.
6. Martin-Vega A and Cobb MH: Navigating the ERK1/2 MAPK cascade. Biomolecules 13: 1555, 2023.
7. Crosbie EJ, Kitson SJ, McAlpine JN, Mukhopadhyay A, Powell ME and Singh N: Endometrial cancer. Lancet 399: 1412-1428, 2022.
8. Shi A, Liu L, Li S and Qi B: Natural products targeting the MAPK-signaling pathway in cancer: Overview. J Cancer Res Clin Oncol 150: 6, 2024.
9. Parvin N, Aslam M, Joo SW and Mandal TK: Nano-phytomedicine: Harnessing plant-derived phytochemicals in nanocarriers for targeted human health applications. Molecules 30: 3177, 2025.
10. Kong X, Zhang R, Shen Y, Bai Y, Dong K, Li D and Wang Y: Preparation and inhibitory effect of salicin dimethyl ether in laryngeal cancer cells through the apoptosis activation. Acta Biochim Pol 69: 753-759, 2022.
11. Kong CS, Kim KH, Choi JS, Kim JE, Park C and Jeong JW: Salicin, an extract from white willow bark, inhibits angiogenesis by blocking the ROS-ERK pathways. Phytother Res 28: 1246-1251, 2014.
12. Samuni Y, Goldstein S, Dean OM and Berk M: The chemistry and biological activities of N-acetylcysteine. Biochim Biophys Acta 1830: 4117-4129, 2013.
13. Ezerina D, Takano Y, Hanaoka K, Urano Y and Dick TP: N-Acetyl cysteine functions as a Fast-acting antioxidant by triggering intracellular H2S and sulfane sulfur production. Cell Chem Biol 25: 447-459.e4, 2018.
14. Tenorio MCDS, Graciliano NG, Moura FA, Oliveira ACM and Goulart MOF: N-acetylcysteine (NAC): Impacts on human health. Antioxidants (Basel) 10: 967, 2021.
15. Schieber M and Chandel NS: ROS function in redox signaling and oxidative stress. Curr Biol 24: R453-R462, 2014.
16. Son Y, Cheong YK, Kim NH, Chung HT, Kang DG and Pae HO: Mitogen-activated protein kinases and reactive oxygen species: How can ROS activate MAPK pathways? J Signal Transduct 2011: 792639, 2011.
17. Blagosklonny MV: Selective protection of normal cells from chemotherapy, while killing drug-resistant cancer cells. Oncotarget 14: 193-206, 2023.
18. Jiang H, Zuo J, Li B, Chen R, Luo K, Xiang X, Lu S, Huang C, Liu L, Tang J and Gao F: Drug-induced oxidative stress in cancer treatments: Angel or devil? Redox Biol 63: 102754, 2023.
19. Gordhandas S, Zammarrelli WA, Rios-Doria EV, Green AK and Makker V: Current evidence-based systemic therapy for advanced and recurrent endometrial cancer. J Natl Compr Canc Netw 21: 217-226, 2023.
20. Mahdi H, Chelariu-Raicu A and Slomovitz BM: Immunotherapy in endometrial cancer. Int J Gynecol Cancer 33: 351-357, 2023.
21. Hayes JD, Dinkova-Kostova AT and Tew KD: Oxidative stress in cancer. Cancer Cell 38: 167-197, 2020.
22. Brandl N, Seitz R, Sendtner N, Muller M and Gulow K: Living on the edge: ROS homeostasis in cancer cells and its potential as a therapeutic target. Antioxidants (Basel) 14: 1002, 2025.
23. Aboul-Soud MAM, Ashour AE, Challis JK, Ahmed AF, Kumar A, Nassrallah A, Alahmari TA, Saquib Q, Siddiqui MA, Al-Sheikh Y, *et al*: Biochemical and molecular investigation of in vitro antioxidant and anticancer activity spectrum of crude extracts of willow leaves Salix safsaf. Plants (Basel) 9: 1295, 2020.
24. Nakamura H and Takada K: Reactive oxygen species in cancer: Current findings and future directions. Cancer Sci 112: 3945-3952, 2021.
25. Dho SH, Cho M, Woo W, Jeong S and Kim LK: Caspases as master regulators of programmed cell death: Apoptosis, pyroptosis and beyond. Exp Mol Med 57: 1121-1132, 2025.
26. Galluzzi L, Vitale I, Aaronson SA, Abrams JM, Adam D, Agostinis P, Alnemri ES, Altucci L, Amelio I, Andrews DW, *et al*: Molecular mechanisms of cell death: Recommendations of the nomenclature committee on cell death 2018. Cell Death Differ 25: 486-541, 2018.
27. Ausina P, Branco JR, Demaria TM, Esteves AM, Leandro JGB, Ochioni AC, Mendonca APM, Palhano FL, Oliveira MF, Abou-Kheir W, *et al*: Acetylsalicylic acid and salicylic acid present anticancer properties against melanoma by promoting nitric oxide-dependent endoplasmic reticulum stress and apoptosis. Sci Rep 10: 19617, 2020.
28. Perillo B, Di Donato M, Pezone A, Di Zazzo E, Giovannelli P, Galasso G, Castoria G and Migliaccio A: ROS in cancer therapy: The bright side of the moon. Exp Mol Med 52: 192-203, 2020.
29. Liu J, Liu Q, Han J, Feng J, Guo T, Li Z, Min F, Jin R and Peng X: N-acetylcysteine inhibits patulin-induced apoptosis by affecting ROS-mediated oxidative damage pathway. Toxins (Basel) 13: 595, 2021.

30. Bahar ME, Kim HJ and Kim DR: Targeting the RAS/RAF/MAPK pathway for cancer therapy: From mechanism to clinical studies. Signal Transduct Target Ther 8: 455, 2023.
31. Aldini G, Altomare A, Baron G, Vistoli G, Carini M, Borsani L and Sergio F: N-acetylcysteine as an antioxidant and disulphide breaking agent: The reasons why. Free Radic Res 52: 751-762, 2018.